

Intense femtosecond shaped laser beams for writing extended structures inside transparent dielectrics

Pavel Polynkin

Received: 18 September 2013 / Accepted: 29 October 2013 / Published online: 14 November 2013
© Springer-Verlag Berlin Heidelberg 2013

Abstract We review recent results on the propagation and self-focusing of intense femtosecond laser pulses with shaped beam profiles in transparent dielectric media. At sufficiently high optical power, beam shaping seeds into the transverse modulation instability and results in the deterministic placement of intense laser filaments within the beam profile. Resulting spatial filament distributions may be utilized for writing complex extended structures inside transparent dielectrics. Specific examples of beam shapes we will discuss are Bessel beams, optical vortices, Bessel beams of higher order, and Airy beams.

1 Introduction

Writing extended index structures by ultrashort pulse lasers inside transparent dielectric media often requires the application of pulses with high energy per pulse. The peak pulse power which scales as the ratio of the pulse energy to the pulse duration, in that case may be many times the power threshold for self-focusing in the material. For common transparent dielectrics such as glasses and transparent liquids, in the near-infrared wavelength range, the value of the critical power is in the several Megawatt range and scales inversely proportional to the optical wavelength of excitation squared. For a smooth bell-shaped input laser beam with peak laser power one to several times above the self-focusing threshold, the transverse beam dimension contracts on propagation due to self-focusing until the intensity reaches the level high enough for enabling an

additional highly nonlinear effect that prevents the beam from collapsing all the way to a singularity. In the case of transparent solids or liquids this highly nonlinear effect is the spectral broadening of the pulse combined with material dispersion which breaks the spectrally broadened laser pulse into sub-pulses. The pulse splitting event may occur several times along the propagation distance, if the input laser power is high enough. The associated temporal pulse dynamics is quite complex. In general, the on-set of self-focusing in the case when writing smooth extended in-volume structures is the goal, is undesirable. The underlying physics is highly nonlinear and therefore small fluctuations of the input power of the laser pulse lead to large variations in size and morphology of the resulting structural modifications inside the material.

If the input pulse power is many times the critical threshold power and the input beam profile is perfectly or nearly perfectly smooth, the transverse modulation instability driven by self-focusing breaks the beam up into multiple hot spots or filaments that are placed randomly within the beam profile [1]. Complex temporal dynamics involving pulse splitting happens within each filament, making the resulting spatio-temporal evolution of the laser beam excessively complex and unrepeatable from one laser shot to another. It has been realized early on the studies of laser filamentation, that the randomness of the transverse filament placement can be overcome and the placement of filaments within the beam profile can be effectively controlled through the introduction of amplitude or phase intensity modulation onto the intense input beam [2]. The hot spots in the beam seed into the transverse modulation instability and determine where filaments are formed. Since the original proposal of [2], beams shaping as the means of control over laser filamentation has been extensively investigated. A wide variety of beams can be generated through phase-only modulation,

P. Polynkin (✉)
College of Optical Sciences, The University of Arizona,
1630 East University Blvd., Tucson, AZ 85721, USA
e-mail: ppolynkin@optics.arizona.edu

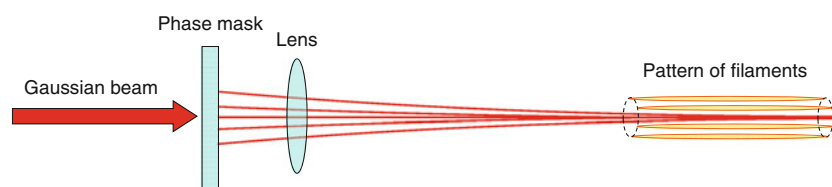


Fig. 1 Generic setup for the generation of various shaped beams. The smooth phase front of the incident laser beam passes through a phase mask and is subsequently focused by a lens or curved mirror. The desired beam shape is realized in the vicinity of the focal plane of the focusing optic

followed by Kirchhoff or Fourier transformation, either through the propagation of the beam into the far field or through focusing the beam with a lens or a curved mirror. In that case, beam shaping is not accompanied by loss of optical power, which is different from the case when amplitude modulation is used. The generic setup for the generation of shaped beams through phase modulation is shown in Fig. 1. The phase mask utilized to impose a particular phase-front modulation onto the incident beam may be either static or programmable (e.g., liquid crystal based).

Examples of beams that can be produced through the combination of phase-only modulation and focusing include Bessel beams, vortex beams, Bessel beams of higher order and Airy beams. All of the above have been realized in the regime of optical power sufficiently high to result in self-focusing and filamentation. Some of these beams have been utilized for writing extended index structures in transparent dielectrics. In what follows, we will review recent results on the generation of these beams and the applications of these beams for processing of transparent materials.

For experimental studies of self-focusing of ultrafast high-power laser beams in condensed media, in the regime of single-shot interaction, transparent liquids offer a convenient substitute for glasses, as at reasonable pulse repetition rates of up to hundreds of kilohertz, a liquid sample does not have to be translated between laser shots. A liquid medium self-heals to a fresh state at the interaction site between laser shots, while a transparent solid has to be translated to a fresh location from one laser shot to another, in order for the interaction to proceed in the single-shot regime. At the same time, the propagation dynamics of ultra-intense and ultrashort laser pulses in transparent solids and liquids are very similar, as the key physical material parameters, such as the critical power for self-focusing, dispersion, and ionization rates are of the same orders of magnitude in essentially all transparent materials, in which the frequency of the resonant optical transition lines is far from the optical frequency of the excitation laser.

2 Bessel beams

Bessel beams are known and utilized in linear optics for many years [3]. In a linear medium, these beams represent

a particular solution of the wave equation that remains invariant on propagation, i.e., propagates diffraction-free. An ideal diffraction-free Bessel beam has its transverse amplitude beam profile described in terms of the Bessel function of zero order. Such a beam profile is not square integrable, which means that it carries infinite power. Consequently, ideal Bessel beams cannot be realized experimentally. However, truncated or apodized Bessel beams, that can be realized, retain certain diffraction-free properties. The characteristic property of these beams is the existence of an intense central lobe within the beam profile. If the beam propagates linearly, the central lobe remains approximately unchanged on propagation over the propagation range that is determined by the input beam size. Interestingly, the beam maintains this property even under a moderately nonlinear propagation, as will be discussed below. The propagation distance over which the beam propagates approximately diffraction-free is commonly referred to as the linear focus zone. In practice, truncated Bessel beams are produced through focusing a flat-top or a Gaussian beam with a conical lens called axicon [4]. The extent of the linear focus zone in this case is determined by the conical angle of the beam and the input beam diameter.

The extended diffraction-free propagation of a Bessel beam enables the writing of line-type structures with high aspect ratios inside transparent solids [5]. In this case, the peak intensity of the central lobe of the beam may be sufficient to support nonlinear propagation, while the periphery of the beam is still propagating linearly. This is a practically interesting regime, in which the continuous nonlinear losses in the central lobe of the Bessel beam are replenished through the radial in-flow of energy from the peripheral part of the beam. Even though the propagation of the central lobe may be highly nonlinear, the shape of the lobe is maintained over extended propagation distances. The supporting peripheral beam structure which is propagating linearly effectively re-heals not only the effects of diffraction of the central lobe, but also those of linear and nonlinear losses.

Highly nonlinear propagation of femtosecond Bessel beams has been studied in gaseous media. Ultra-intense femtosecond Bessel beams with the pulse energy in tens of millijoules have been applied for the generation of meters-long plasma filaments in air and other gasses [6]. Such

experiments have shown that, under certain conditions, nonlinear optical interactions within the intense Bessel zone lead to the efficient generation of an intense and broadband radiation propagating on the beam axis [9]. In the case of self-focusing and filamentation of intense laser beams in a gas, certain propagation parameters can be monitored in-situ through, for example, the measurements of the density of plasma that is left in the wake of the laser pulse [7] or through monitoring plasma fluorescence [8].

3 Vortex beams

An optical vortex is another example of a shaped beam that can be generated from a flat-top or a Gaussian input beam through the application of phase-only beam modulation. The required phase profile in this case is in the form $\propto \exp(im\phi)$, where ϕ is the azimuthal angle and m is the order of the vortex, also known as the topological charge. Since in practice the maximum depth of phase modulation of common phase masks is limited, vortex phase masks, like other types of phase masks, are usually made *modulo*- 2π . Vortex beams have doughnut-shaped intensity distributions. Under fixed focusing conditions, the diameter of the intensity ring grows approximately linearly with the vortex order. An example of the phase profile of a mask used to generate an optical vortex of order 8 is shown in Fig. 2, together with the photographs of intensity patterns of experimentally generated optical vortices of orders 3, 6, and 10.

An important property of vortex beams is the orbital angular momentum of $m\hbar$ carried by every photon

comprising the vortex beam of order m . This momentum can be used to spin microscopic particles suspended in liquids [10].

The interest in the studies of optical vortices has been in part fueled by the fact that these beams are resistant to self-focusing collapse and therefore can be used to transmit high-power optical beams over long distances. It has been found through the approximate solution of the nonlinear Schrodinger equation that the critical power for the self-similar collapse of a continuous-wave vortex beam of order m approximately equals $2\sqrt{3}m \cdot P_{cr}^{(0)}$, where $P_{cr}^{(0)}$ is the critical power for self-focusing of a Gaussian beam [11].

Recent developments of the technology for fabrication of large-area thin glass phase masks allowed for the demonstration of vortex beams of various orders in the short-pulse, ultra-intense regime [12]. It has been shown that even in the femtosecond case, the resistance of optical vortices to self-focusing persists. However, when the collapse happens at high enough laser intensity, the beam does not collapse self-similarly (i.e., while maintaining its smooth doughnut-shaped intensity profile). Instead, the intensity ring fragments into individual filaments that populate the intensity ring and rotate on propagation (Fig. 3).

The fragmentation of the vortex ring into filaments as the dominant mode of self-focusing collapse has been considered in [13] and experimentally demonstrated, for vortices of orders 1 and 2 [14]. In [12], these results have been extended onto the cases of vortices of higher orders.

The rotation rate of the filament pattern resulting from self-focusing collapse of an optical vortex beam can be estimated based on the following mechanical argument.

Fig. 2 Left 2π -modulo phase pattern used to generate optical vortex of order 8. Right doughnut-shaped intensity profiles for optical vortices of selected orders, as indicated in the individual subfigures

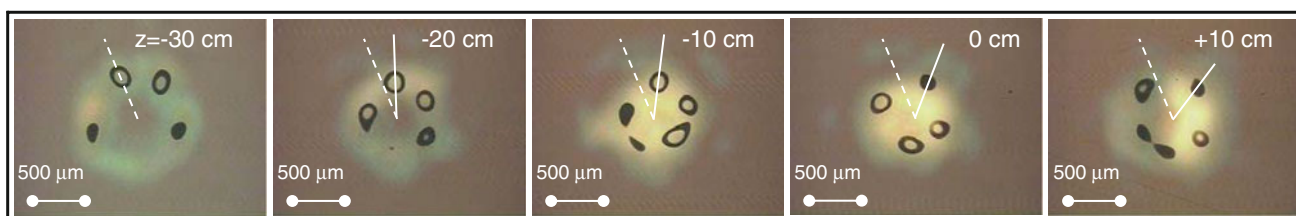
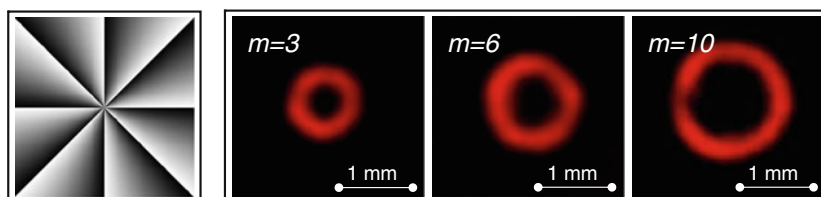


Fig. 3 Several snapshots of the ring filament patterns generated in air through self-focusing of an intense femtosecond optical vortex of order 3. The patterns are obtained through photographing single-shot burns produced by the beam on a smooth plastic surface. As the

intense beam self-focuses and propagates, the filament pattern rotates in the direction determined by the sense of vorticity. The rate of this rotation can be accurately estimated based on a simple mechanical argument, as discussed in the text

Consider the photon in the optical vortex of order m as a particle with “mass” M , propagating along a spiral trajectory of radius R with the forward drift velocity equal to the speed of light c . The ratio of the angular and linear momenta for such a particle equals $M \cdot \Omega R^2 / (M \cdot c)$, where Ω is the revolution rate of the particle around its spiral trajectory, in radians per second. The ratio of the angular and linear momenta for an actual photon in the vortex beam of order m is $\hbar \cdot m / (\hbar \cdot k)$, where k is the wave-number. Equating the two ratios, for the rotation rate per unit path length we find: $\Omega/c = m \cdot \lambda / (2\pi R^2)$, where λ is the wavelength. R stands for the radius of the ring filament pattern. The photon “mass” M cancels out from the result, as expected. Since the radius of the vortex ring is approximately proportional to the vortex order, the overall dependence of the rotation rate on the order of the vortex is inverse, at fixed focusing conditions. For the case shown in Fig. 3, the measured rotation rate is $(1.7 \pm 0.2)^\circ/\text{cm}$, close to the estimation according to the above formula.

The application of vortex beams to femtosecond laser machining of glass surfaces has been recently reported [15]. Depending on the pulse energy, femtosecond vortices of order 2 have been shown to produce ablation marks with different morphology. Under certain conditions, a deep cavity was formed on the beam axis, where the beam intensity has a minimum. The radial implosion driven by the tightly focused femtosecond vortex beam has been suggested as a possible mechanism of the void formation. In the case of in-volume laser machining, optical vortices may enable writing of extended bottle-like waveguide structures in transparent materials. As of time of this writing, the details of the interaction of intense femtosecond vortex beams with materials are not fully understood and are the subject of intense investigations.

4 Bessel beams of higher order

These beams are produced though the phase modulation of an input flat-top or Gaussian beam with the modulation function in the form:

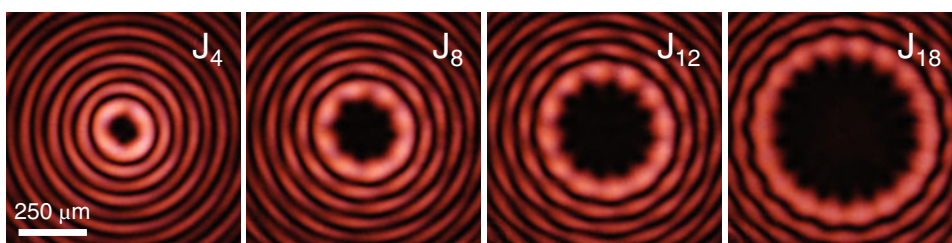
$$T_n(r, \theta) = \exp(in\theta) \cdot \exp\left(-\frac{2\pi ir}{r_0}\right), \quad (1)$$

where n is the order of the beam, (r, θ) are transverse polar coordinates, and r_0 is a scale factor. In the above formula, the first exponential factor is identical to the one that stands in the phase profile of an optical vortex, and the second exponential is the same as the one produced by the axicon lens used to generate a fundamental Bessel beam. The resulting transverse amplitude of the beam is proportional to $J_n(2\pi r/r_0) \cdot \exp(in\theta)$. The beam intensity profile is in the form of concentric rings. Like vortex beams, Bessel beams of higher order carry a topological charge. And like fundamental Bessel beams, Bessel beams of higher order are approximately diffraction-free, which means that they maintain their dominant ring intensity features over extended propagation distances.

Intense femtosecond Bessel beams of higher order have been recently realized and their propagation properties in a transparent dielectric medium have been studied [16]. In these experiments, the phase modulation was imposed via a programmable liquid crystal-based spatial light modulator (SLM). Due to the calibration offset of the SLM, the ring intensity features in the generated beams, supposed to be smooth for ideal higher-order Bessel beams, were instead beaded, as shown in Fig. 4.

As the input pulse energy was increased, the onset of self-focusing of the higher-order Bessel beams resulted in the fragmentation of the dominant ring intensity features of the beams into individual intense filaments. Filamentation was seeded by the hot spots in the modulated input beam profiles, resulting in the generation of regular ring patterns of filaments. Each filament sourced a bright forward-propagating white-light supercontinuum, as shown in Fig. 5 (top row). As the energy of the laser pulses was increased further, the secondary ring features became intense enough to produce filaments. The resulting concentric patterns of filaments are shown in Fig. 5 (bottom row). Such filament patterns, in principle, can be used for writing extended waveguiding structures inside transparent dielectric materials, similar to those in micro-structured optical fibers.

Fig. 4 Transverse intensity profiles of experimentally generated higher-order Bessel beams for several selected beam orders. The ring intensity features of the beams are beaded due to the wavelength offset of the spatial light modulator used to generate these beam shapes



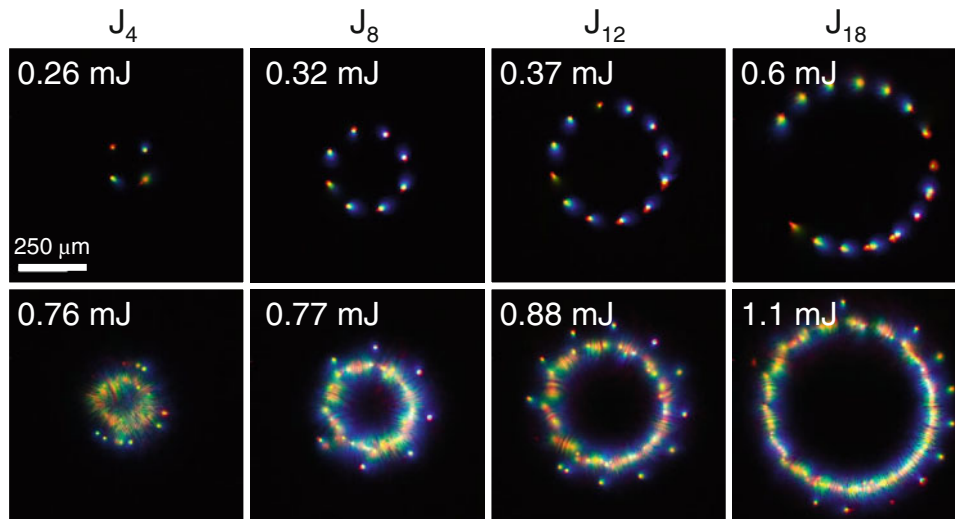


Fig. 5 Patterns of white-light supercontinuum emission resulting from self-focusing and filamentation of higher-order Bessel beams of selected orders in water. *Top row* the dominant (central) ring feature has sufficient power to produce filaments, while secondary ring features have insufficient power for filamentation. One ring of

regularly spaced filaments is produced in this case. *Bottom row* the beam energy is sufficient for both the dominant and the secondary ring features to produce filaments. Filament structures of this kind can be potentially used for writing extended waveguiding structures inside transparent dielectrics

5 Airy beams

Airy beams represent a new class of accelerating optical beams recently introduced to optics [17]. The transverse amplitude profile of these beams is described in terms of the two-dimensional Airy function:

$$E(x, y) \propto Ai(x/B)Ai(y/B) \exp\left(a \frac{x+y}{B}\right), \quad (2)$$

where (x, y) are the transverse Cartesian coordinates, B is a scale factor, and a is the so-called confinement parameter. As for an ideal Bessel beam, the ideal (not confined) Airy beam, which corresponds to the case $a = 0$ in the formula above, is not square integrable. The inclusion of the exponential factor in the definition above ensures that the beam has finite energy and is thus experimentally realizable. Note that since Airy function extends indefinitely into the negative values of its argument, the confinement parameter a is a positive number. Smaller values of a correspond to larger values of energy carried by the confined Airy beam.

Like all beam examples considered here, an Airy beam is generated from a flat-top or a Gaussian beam through phase-only modulation of the phase front of the input beam. The phase modulation in this case follows a cubic dependence in x and y coordinates as follows:

$$T_n(r, \theta) = \exp\left[i \frac{\beta}{3} (x^3 + y^3)\right], \quad (3)$$

where β is a scale factor. The parameters of thus generated Airy beam are related to the parameters of the input

Gaussian beam and the scale factor of the phase mask. The example phase profile of the cubic phase mask, *modulo-2* π , used to generate an Airy beam, as well as the illustration of the transverse beam profile are shown in Fig. 6. The beam profile has a prominent peak in the corner of the beam pattern. The two main properties of this type of a beam structure are that the peak propagates along a curved trajectory and the propagation is approximately diffraction-free. Similar to the case of a Bessel beam, the diffraction-resistant propagation of the dominant intensity feature of the beam is a result of diffraction that continuously rebuilds this feature at the expense of energy provided by the supporting peripheral beam structure.

Airy beams have been experimentally demonstrated in the linear-optic regime (at low intensity) in [17]. In that original demonstration, the curvature of the beam

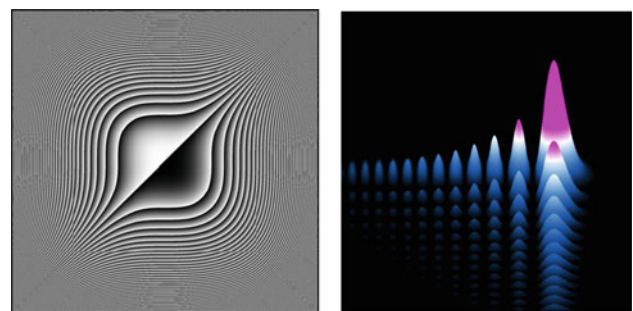


Fig. 6 *Left* phase profile of a cubic phase mask, *modulo-2* π used to generate an Airy beam pattern. *Right* illustration of the transverse intensity profile of an Airy beam

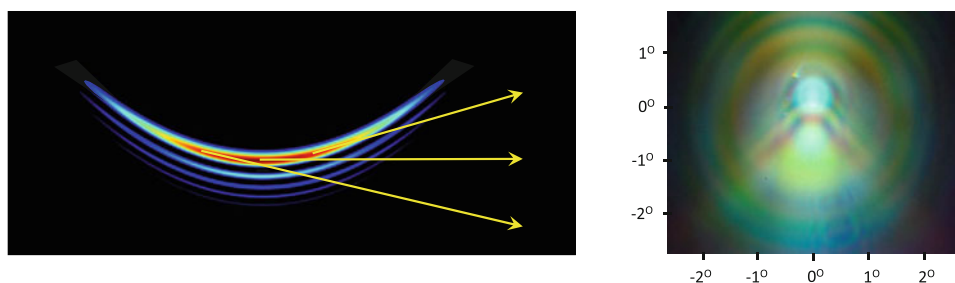


Fig. 7 *Left* self-bending trajectories traversed by the dominant intensity features of an Airy beam. *Right* far-field intensity patterns of the white-light supercontinuum generated by intense femtosecond

trajectories was a fraction of one degree, which was quite modest. The concept of Airy beams has been later generalized onto the non-paraxial case, and beam deflections as high as 90° have been shown to be feasible [18].

Airy beams have been realized in the realm of femtosecond, ultra-intense nonlinear optics, both in a gas [19] and in a transparent condensed medium [20]. In the propagation regimes that support nonlinear self-focusing, the transverse collapse of the dominant intensity feature of the beam results in the generation of forward-propagating white-light supercontinuum emission. The emissions originating at different points along the beam path propagate along angularly resolved trajectories, as illustrated in Fig. 7. This feature may enable longitudinally resolved remote sensing, as discussed in [21].

Very recently, the application of self-bending Airy beams to material processing has been reported [22]. The accelerating and self-healing properties of these beams provide an additional degree of control over the geometry of the machined structures and enable the fabrication of trenches with smooth-curved edges in transparent dielectric materials. The intensity of the beam in this case can be adjusted so that only the dominant intensity peak of the beam is intense enough to ablate the material, while the supporting beam structure propagates in the nearly linear regime, facilitating the extended diffraction-free propagation and the formation of curved trenches with high aspect ratios.

6 Conclusion

In conclusion, we have discussed recent experiments on the generation and application of intense femtosecond laser pulses with shaped beam fronts. In the case of laser machining of extended structures inside transparent dielectric materials, high-power laser pulses are typically used, in which case the transverse beam reshaping and filamentation due to self-focusing become relevant. In that case, beam shaping can be successfully used as a means of

Airy beams propagating in water. The presence of several vertically displaced bright spots in the pattern is indicative of multiple self-focusing collapse events of the dominant intensity feature of the beam

control over the placement of intense filaments within the beam profile, resulting in the formation of regular filament structures with particular properties. The examples of intense-shaped beams considered in this review included Bessel beams, vortex beams, Bessel beams of higher order and Airy beams.

Acknowledgments The author acknowledges helpful discussions with Demetrios Christodoulides and Miroslav Kolesik. The preparation of this review article was supported by the United States Air Force Office of Scientific Research (U.S. AFOSR) through grants No. FA9550-12-1-0482, No. FA9550-12-1-0143, and No. FA9550-10-1-0561.

References

- Mlejnek M, Kolesik M, Moloney J, Wright E (1999) Optically turbulent femtosecond light guide in air. *Phys. Rev. Lett.* 83:2938
- Mechain G, Couairon A, Franco M, Prade B, Mysyrowicz A (2004) Organizing multiple femtosecond filaments in air. *Phys. Rev. Lett.* 93:035003
- Durmin J, Miceli J, Eberly J (1987) Diffraction-free beams. *Phys. Rev. Lett.* 58:1499
- McLeod J (1954) The axicon: a new type of optical element. *J. Opt. Soc. Am.* 44:592
- Bhuyan M, Courvoisier F, Lacourt P, Jacquot M, Salut R, Furtaro L, Dudley J (2010) High aspect ratio nanochannel machining using single shot femtosecond Bessel beams. *Appl. Phys. Lett.* 97:081102
- Polynkin P, Kolesik M, Roberts A, Faccio D, Di Trapani P, Moloney J (2008) Generation of extended plasma channels in air using femtosecond Bessel beams. *Opt. Express* 16:15733
- Polynkin P (2012) Mobilities of O_2^+ and O_2^- ions in femtosecond laser filaments in air. *Appl. Phys. Lett.* 101:164102
- Bernhardt J, Liu W, Theberge F, Xu H, Daigle J, Chateaufneuf M, Dubois J, Chin SL (2008) Spectroscopic analysis of femtosecond laser plasma filament in air. *Opt. Commun.* 281:1268
- Polynkin P, Kolesik M, Moloney J (2009) Extended filamentation with temporally chirped femtosecond Bessel-Gauss beams in air. *Opt. Express* 17:575
- He H, Friese M, Heckenberg N, Rubinsztein-Dunlop H (1995) Direct observation of transfer of angular momentum to absorptive particles from a laser beam with a phase singularity. *Phys. Rev. Lett.* 75:826
- Fibich G, Gavish N (2008) Critical power of collapsing vortices. *Phys. Rev. A* 77:045803

12. Polynkin P, Ament C, Moloney J (2013) Self-focusing of ultra-intense femtosecond optical vortices in air. *Phys. Rev. Lett.* 111:023901
13. Vincotte A, Berge L (2005) Femtosecond optical vortices in air. *Phys. Rev. Lett.* 95:193901
14. Vuong LT, Grow TD, Ishaaya A, Gaeta AL, 't Hooft GW, Eliel ER, Fibich G (2006) Collapse of optical vortices. *Phys. Rev. Lett.* 96:133901
15. Hnatovsky C, Shvedov V, Krolikowski W, Rode A (2010) Materials processing with a tightly focused femtosecond laser vortex pulse. *Opt. Lett.* 35:3417
16. Shiffler S, Polynkin P, Moloney J (2011) Self-focusing of femtosecond diffraction-resistant vortex beams in water. *Opt. Lett.* 36:3834
17. Siviloglou G, Broky J, Dogariu A, Christodoulides D (2007) Observation of accelerating Airy beams. *Phys. Rev. Lett.* 99:213901
18. Kaminer I, Bekenstein R, Nemirowsky J, Segev M (2012) Non-diffracting accelerating wave packets of Maxwell's equations. *Phys. Rev. Lett.* 108:163901
19. Polynkin P, Kolesik M, Moloney J, Siviloglou G, Christodoulides D (2009) Curved plasma channel generation using ultraintense Airy beams. *Science* 324:229
20. Polynkin P, Kolesik M, Moloney J (2009) Filamentation of femtosecond laser Airy beams in water. *Phys. Rev. Lett.* 103:123902
21. Polynkin P, Kolesik M, Moloney J, Siviloglou G, Christodoulides D (2010) Extreme nonlinear optics with ultra-intense self-bending Airy beams. *Opt. Photon. News* 21:38
22. Mathis A, Courvoisier F, Froehly L, Furfaro L, Jacquot M, Lacourt P, Dudley J (2012) Micromachining along a curve: femtosecond laser micromachining of curved profiles in diamond and silicon using accelerating beams. *Appl. Phys. Lett.* 101:071110